JOC The Journal of Organic Chemistry

Article

pubs.acs.org/joc

The Design and Synthesis of Alanine-Rich α-Helical Peptides Constrained by an *S,S*-Tetrazine Photochemical Trigger: A Fragment Union Approach

Joel R. Courter, Mohannad Abdo, Stephen P. Brown, Matthew J. Tucker,[†] Robin M. Hochstrasser,[‡] and Amos B. Smith, III*

Department of Chemistry, University of Pennsylvania, Philadelphia, Pennsylvania 19104, United States

Supporting Information

ABSTRACT: The design and synthesis of alanine-rich α-helical peptides constrained in a partially unfolded state by incorporation of the *S,S*-tetrazine phototrigger has been achieved, permitting, upon photochemical release, observation by 2D-IR spectroscopy of the subnanosecond conformational dynamics that govern the early steps associated with α-helix formation. Solid-phase peptide synthesis was employed to elaborate the requisite fragments, with full peptide construction via solution-phase fragment condensation. The fragment union tactic was also employed to construct $^{13}C{=}^{18}O$ isotopically edited amides to permit direct observation of conformational motion at or near specific peptide bonds.

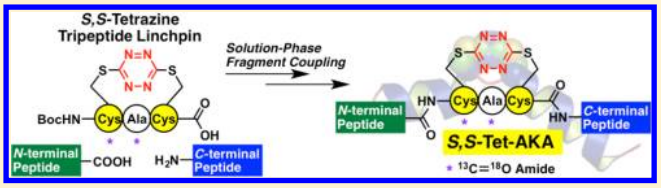

INTRODUCTION

Peptides and proteins comprise dynamic entities that, in many cases, exploit conformational changes and/or transient molecular interactions to achieve their biological function.[1−5] Understanding the early kinetic events that govern conformational dynamics in peptides, and in turn proteins, is critical for the development and refinement of models that relate dynamic structure to the observed biological function.[6−8] Structural snapshots of such biomolecules can be achieved at atomic resolution by X-ray crystallography and nuclear magnetic resonance measurements. However, these static structures do not provide information on transiently sampled nonequilibrium structures. Structural change on the millisecond time scale can be defined by nuclear magnetic resonance spectroscopy,[9] while advances in time-resolved X-ray crystallography[10−14] permit temporal resolution on subnanosecond time scales within a crystal, although this approach remains technically challenging. Two-dimensional infrared (2D-IR) spectroscopy, developed and pioneered by Hochstrasser and colleagues,[15−17] in conjunction with ultrafast photochemical release (i.e., triggering),[5,18,19] provides an attractive alternative method to initiate and subsequently observe the earliest kinetic processes associated with conformational change (i.e., protein folding and misfolding). For example, incorporation of a phototrigger to confine a peptide/protein within a narrow distribution of conformers, followed by ultrafast photochemical release of the geometric constraint, would permit precise temporal control. In particular, the peptide conformation would evolve, with some initial spatial coherence, toward a different distribution, ultimately reaching the native equilibrium distribution of peptide/protein conformations.

Previously developed phototriggers include non-native disulfide bonds, pioneered by Hochstrasser and DeGrado,[20,21] and the methoxybenzoin-based systems developed by Chan and co-workers.[22−25] However, these triggers have limitations, including rapid recombination of the initial photoproducts,[20,26] the inherent chemical reactivity of the derived photoproducts, and, in the case of methoxybenzoin-based systems, the introduction of obtrusive non-native chemical appendages as a result of the phototrigger structure. Criteria for the ideal phototrigger, as previously defined,[18] include (1) photochemical fragmentation on a time scale shorter than the conformational changes under observation, (2) a reasonably high photochemical yield, (3) inert products with negligible side reactions along the photochemical pathway, (4) functionality permitting ready incorporation within peptides and proteins, (5) sufficient stability to permit synthetic manipulations and purification both in solution and on solid supports, and (6) photochemical cleavage at light frequencies compatible with the amide backbone and amino acid side chains.

To meet these criteria, we introduced the *S,S*-tetrazine chromophore (Figure 1A).[27−29] Importantly, the photoproducts comprise inert and unobtrusive thiocyanates and nitrogen; moreover, the *S,S*-tetrazine phototrigger can be inscribed readily between two cysteine residues to constrain a peptide within a narrow distribution of conformers.[28] We also described UV-pump transient 2D-IR-probe experiments to monitor the structural relaxation of a 24 residue alanine-rich peptide containing a kink induced by the *S,S*-tetrazine phototrigger (Figure 1B).[30] Upon release of the constraint,

Received: December 3, 2013
Published: December 20, 2013

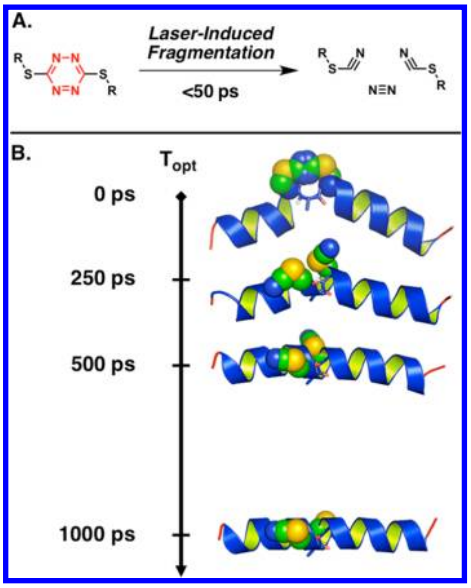

Figure 1. (A) Photolysis of the *S,S*-tetrazine phototrigger can be achieved with laser pulses at various wavelengths that afford two thiocyanates and molecular nitrogen in less than 50 ps. (B) Schematic representation of *S,S*-tetrazine phototriggering applied to ***S,S*-Tet-AKA**. Photolysis of the *S,S*-tetrazine (shown in space-filling representation) removes the structural constraint to furnish the bis-SCN peptide photoproduct. The 2D-IR measurements at various time delays following the photolysis pulse (T_{opt}) directly monitor the conformational relaxation within the central CAC motif (the main chain of the peptide in the CAC region is shown in sticks).

initiated by a subpicosecond pulse of UV irradiation (λ = 355 nm), the formation of a single α-helix turn was directly observed by 2D-IR spectroscopy without "unzipping" of nearby helix turns (vide infra).

Herein we describe the design and requisite synthesis of a constrained 24-residue alanine-rich α-helical peptide possessing the *S,S*-tetrazine phototrigger (***S,S*-Tet-AKA**; cf. Figure 2) by means of a solution-phase fragment coupling tactic. The synthesis of $^{13}C{=}{=}^{18}O$ edited isotopomers is also described.[30] Going forward, the general fragment coupling protocol developed to construct ***S,S*-Tet-AKA** can now be applied to peptides and proteins of greater complexity to initiate conformational changes that occur on subnanosecond time scales.

RESULTS AND DISCUSSION

Design and Synthesis. We initiated studies to construct peptides containing the *S,S*-tetrazine within the 24-residue alanine-rich **AKA** peptide (Figure 2), a system introduced by Baldwin and colleagues[31] to adopt in the ground state an α-helical structure that has subsequently often been employed in folding and relaxation studies. We reasoned that introduction of the *S,S*-tetrazine moiety within the middle of a 24-residue peptide would permit both the *N*- and *C*-terminal segments to maintain an α-helical conformation, while the amino acids between the cysteine residues would remain nonhelical because of the geometric constraints enforced by incorporation of the *S,S*-tetrazine phototrigger (Figure 1B). Upon photochemical release of the constraint imposed by the *S,S*-tetrazine phototrigger, the terminal α-helices would direct the central kinked residues to equilibrate rapidly to the preferred extended α-helical conformation. In contrast to peptide "stapling", wherein the introduced cross-link(s) typically aim to introduce minimal changes to the ground-state conformation of the peptide,[32] we require the *S,S*-tetrazine "staple" to introduce a well-defined local perturbation to the peptide conformation. Of interest, the *S,S*-tetrazine staple can be rapidly released upon photolysis.

A variety of (i, i + 2/4) spacings between the cysteine residues inscribing the *S,S*-tetrazine system were initially investigated by molecular dynamics (MD) simulations, with distance constraints between the sulfur atoms employed to model the phototrigger.[30] The resultant constrained MD simulations predicted that the ***S,S*-Tet-AKA** peptide would assume a kinked α-helical conformation wherein the *S,S*-tetrazine moiety would disrupt the helical structure between Cys10 and Cys12 (cf. Figure 1B, T_{opt} = 0 ps).[30] Our synthetic targets thus became ***S,S*-Tet-AKA** and isotopically edited versions thereof (Figure 2).

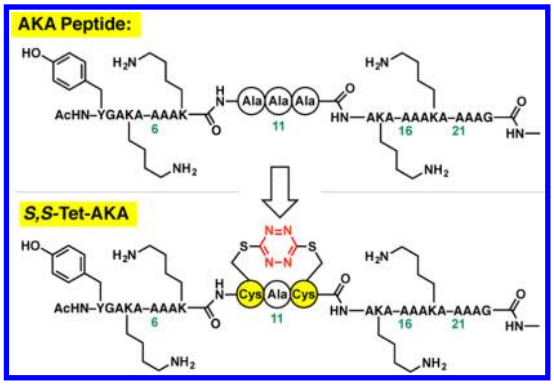

Figure 2. The AKA peptide (top) was employed for the design of an *S,S*-tetrazine-constrained synthetic target, ***S,S*-Tet-AKA** (bottom).

By constraining the center of an α-helix with an *S,S*-tetrazine moiety, we envisioned a perturbation not dissimilar to that induced by a proline residue.[33] To estimate the potential helicity of the designed target peptides relative to the original **AKA** peptide (Scheme 1), model peptides $\mathbf{AKA_{A11P}}$ and $\mathbf{AKA_{A10C/A12C}}$ were constructed via solid-phase peptide syn-

Scheme 1. Synthesis of the AKA Variants $\mathbf{AKA_{A11P}}$ and $\mathbf{AKA_{A10C/A12C}}$

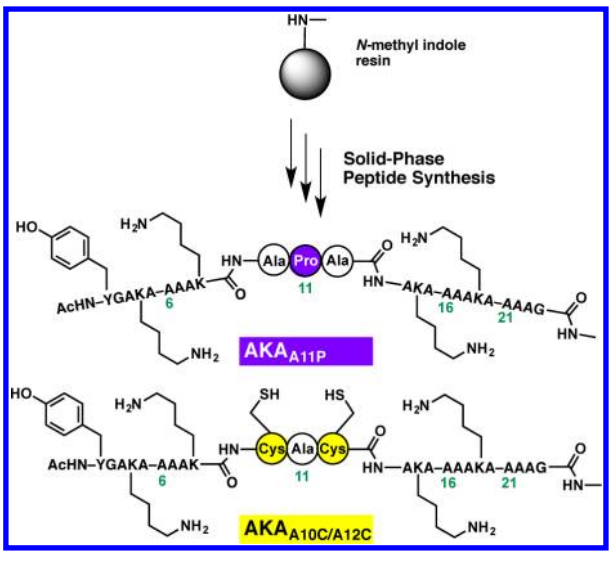

dx.doi.org/10.1021/jo402680v | J. Org. Chem. 2014, 79, 759–768

thesis (SPPS) employing *N*-methylindole aminomethyl resin. The proline mutant **AKA$_{A11P}$** was specifically constructed to mimic the *S*,*S*-tetrazine-constrained peptide before photolysis (i.e., ***S*,*S*-Tet-AKA**), while the double cysteine mutant **AKA$_{A10C/A12C}$** was synthesized to mimic the bis-thiocyanate peptide photoproduct.

The far-UV CD spectra of the ***S*,*S*-Tet-AKA** (prepared as described below), **AKA$_{A11P}$**, and **AKA$_{A10C/A12C}$** peptides were recorded; an absorption band at 222 nm, diagnostic of helical structure, was observed for the native **AKA** peptide (Figure 3).[31] The fractional helicity [θ_{222}] of the native **AKA** was

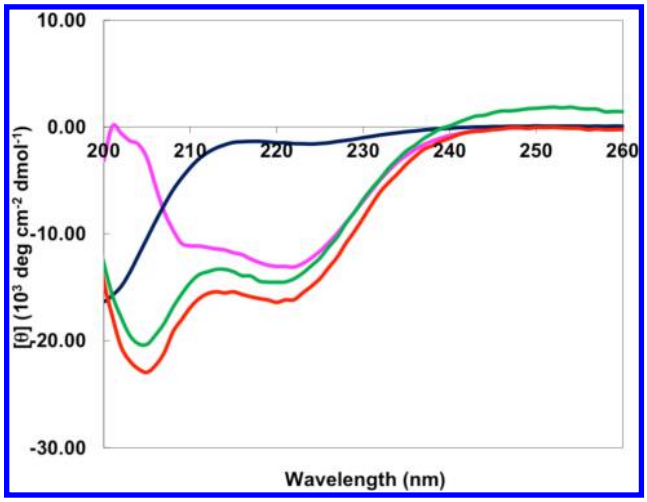

Figure 3. Far-UV CD spectra of **AKA$_{A11P}$** in phosphate buffer (dark blue) and TFE (magenta), **AKA$_{A10C/A12C}$** in TFE (red), and the final synthetic target ***S*,*S*-Tet-AKA** in TFE (green).

determined to be 0.72 in aqueous phosphate buffer (data not shown). The band at 222 nm nearly disappeared upon incorporation of the proline residue within **AKA$_{A11P}$**, suggesting that the fractional helicity was significantly reduced (ca. 0.05).[33] To ensure that a desirable degree of fractional helicity can be achieved for a kinked AKA-type peptide system, trifluoroethanol (TFE), which is known to maximize the peptide helicity and increase the solubility,[34] was employed to enhance the helicity of **AKA$_{A11P}$**. Pleasingly, a value of 0.34 was observed for the **AKA$_{A11P}$** peptide in TFE solution. A slight increase in the fractional helicity to 0.49 was observed for the **AKA$_{A10C/A12C}$** peptide in TFE. These results were highly encouraging, suggesting that following photolysis of the *S*,*S*-tetrazine-constrained AKA peptide (i.e., ***S*,*S*-Tet-AKA**), a more helical conformation should evolve, as suggested by the helicity of the analogous **AKA$_{A10C/A12C}$** peptide indicated by the CD spectra.

Turning to the synthesis of the 24-residue target peptide ***S*,*S*-Tet-AKA**, we recently introduced an SPPS synthetic protocol to incorporate the *S*,*S*-tetrazine phototrigger within short tri-, tetra-, and peptapeptide linchpins.[29] The compatibility of a lysine in the $i + 1$ position relative to the *S*,*S*-tetrazine, however, had not been explored. To validate the compatibly of a protected Lys side chain under the conditions required to insert the *S*,*S*-tetrazine, tetrapeptide **3** was constructed via SPPS, with both the lysine side chain bearing the standard *tert*-butyl carbamate protecting group and with the cysteine side-chain thiols masked with the 4-monomethoxytrityl (Mmt) protecting groups (Scheme 2). The synthesis proceeded without incident. Equally important, we demonstrated that tetrapeptide **3** underwent steady-state photolysis to yield solely bis-thiocyanate peptide **4**, thus confirming that the proximal basic Lys side chain does not perturb the steady-state photolysis of the electron-deficient *S*,*S*-tetrazine. The disappearance of the ^{13}C NMR signals for the tetrazine ring ($\delta_c \approx 170$ ppm) with the concomitant appearance of the SCN resonances at $\delta_c \approx 113$ ppm[27] proved to be particularly diagnostic for monitoring the *S*,*S*-tetrazine photolysis (see the Supporting Information).

Scheme 2. SPPS of Tetrapeptide 3 and Steady-State Photolysis of 3 To Afford Bis-Thiocyante Tetrapeptide 4

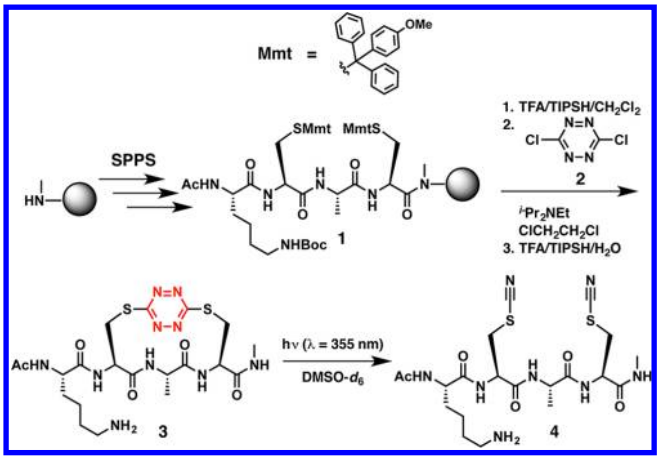

Having achieved the successful construction of a peptide model system and validated the photochemical fragmentation, we turned to the synthesis of ***S*,*S*-Tet-AKA** (Scheme 3). The solid-phase conditions employed earlier to incorporate the *S*,*S*-tetrazine component in the model peptide[27,29] unfortunately proved ineffective when the fully constructed peptide backbone remained immobilized on the solid support. A number of reaction modifications, such as including denaturants, elevating

Scheme 3. Attempted Synthesis of the *S*,*S*-Tet-AKA Peptide on the *N*-Methylindole Solid Support

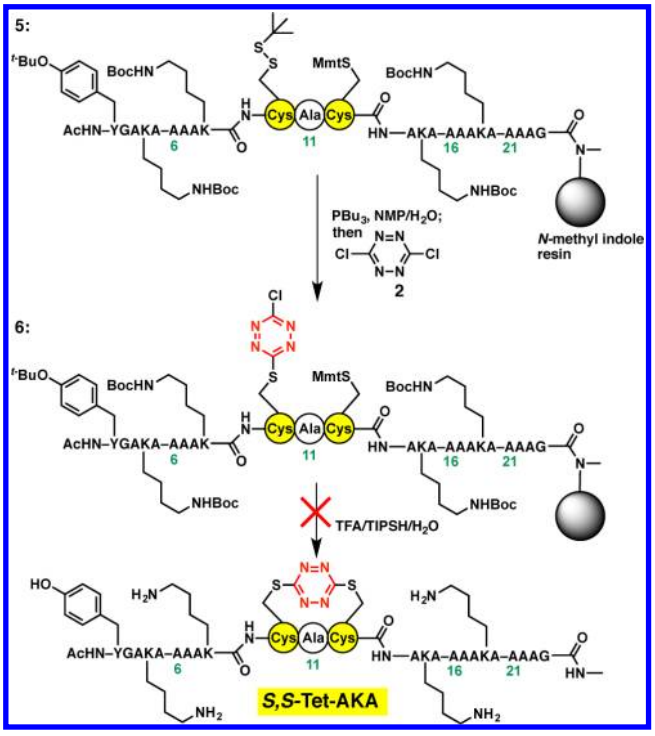

dx.doi.org/10.1021/jo402680v | *J. Org. Chem.* 2014, 79, 759–768

the reaction temperature, or employing more polar solvent systems failed to improve the situation. An alternative synthetic strategy was thus explored wherein orthogonally protected Cys residues[35] [i.e., thio-*tert*-butyl (S^tBu) at Cys10 and Mmt at Cys12] were incorporated during SPPS in an attempt first to introduce the S,Cl-tetrazine (to give **6** in Scheme 3) and then to remove the second thiol protecting group with concomitant formation of the *S,S*-tetrazine moiety. This tactic also proved ineffective. Equally unsuccessful was our tactic employed to replace the disulfide bond in the peptide hormone oxytocin with the *S,S*-tetrazine,[27] which called for treatment of the $\mathbf{AKA}_{\mathbf{A10C/A12C}}$ peptide in an aqueous 0.1 M ammonium bicarbonate solution with dichlorotetrazine (**2**), as this approach also failed to furnish the desired ***S,S*-Tet-AKA** peptide. Presumably the immobilized peptide has a preference to adopt the α-helical structure on the solid support, a conformational bias that could not be sufficiently perturbed to incorporate the *S,S*-tetrazine phototrigger.

Undeterred, we turned to a fragment condensation strategy carried out in solution to construct the ***S,S*-Tet-AKA** peptide. Early studies in our laboratory had demonstrated that the *S,S*-tetrazine moiety is stable toward amide bond coupling protocols.[29] Initially a model system comprising a two-fragment union tactic was explored. To this end, *S,S*-tetrazine peptide **8**, which was readily constructed on the Wang resin with the Lys side chain reprotected as the *tert*-butyl carbamate, furnished coupling partner **9** (Scheme 4A). The requite dodecapeptide coupling partner **10**, corresponding to the *C*-terminal peptide fragment, was next prepared via a standard SPPS protocol. With fragments **9** and **10** in hand, our previously developed fragment union tactic utilizing HBTU and ethyl 2-cyano-2-(hydroxyimino)acetate (oxyma)[29,36] was employed to achieve union at the Cys12−Ala13 amide bond; the yield was 53% (Scheme 4B). Subsequent treatment with TFA furnished peptide **11** in nearly quantitative yield. Importantly, peptide **11** corresponds to residues 7−24 of the full synthetic target ***S,S*-Tet-AKA**.

With construction of the truncated peptide **11** validated, we turned to a three-fragment condensation tactic to generate the target peptide possessing the full *N*-terminal sequence. As the *N*-terminus of our previously reported *S,S*-tetrazine tripeptide linchpin, employed via solution-phase fragment coupling, was most conveniently protected as the Boc carbamate,[29] we sought a semiorthogonal protecting group to mask the lysine side chains. The benzyloxycarbonyl (Cbz) protecting group was selected and proved to be compatible with the *S,S*-tetrazine insertion conditions employed to construct tetrapeptide **13** (Scheme 5A). Importantly, the Cbz protecting groups were retained during removal of **13** from the resin by treatment with TFA/TIPSH/H_2O (95:2.5:2.5) for 2.5−5 h. However, removal of the Cbz protecting group from the Lys side chain to furnish peptide **14** required more strenuous conditions, namely, treatment with TFA for 24 h.

Turning next to the orthogonal Cbz-removal tactic employing hydrogenation, we were surprised to observe rapid loss of the orange color characteristic of the *S,S*-tetrazine chromophore. However, when the colorless solution was permitted to stand exposed to air, the solution slowly regained the original orange color. This observation suggested that hydrogenation had led to semi-reduction of the *S,S*-tetrazine ring. To explore this scenario, we turned to our previously described amino acid-based *S,S*-tetrazine **15** (Scheme 5B).[27] Similar exposure of **15** to the hydrogenation conditions led to loss of the characteristic orange color with formation of dihydro-*S,S*-tetrazine **16** in nearly quantitative yield (^{1}H and ^{13}C NMR). In an effort to

Scheme 4. (A) Preparation of Lys-Protected *S,S*-Tetrazine Hexapeptide 9; (B) Union of *S,S*-Tetrazine Hexapeptide 9 to the *C*-Terminal Peptide Fragment 10 of the *S,S*-Tet-AKA Target Peptide, with the Corresponding Residue Numbers Shown, To Furnish 18-Mer 11

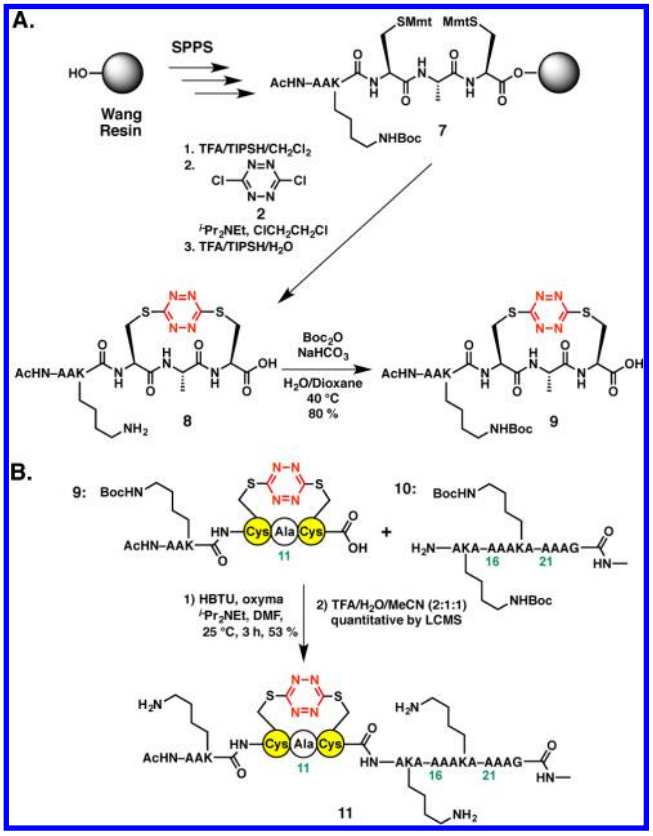

Scheme 5. (A) Evaluation of Benzyloxycarbonyl (Cbz) as an Alternative Protecting Group for the Lysine Side Chain and Validation of the Deprotection Conditions; (B) The *S,S*-Tetrazine Ring of 15 Is Partially Reduced to the Dihydro-*S,S*-Tetrazine System 16 upon Exposure to Hydrogenolysis Conditions

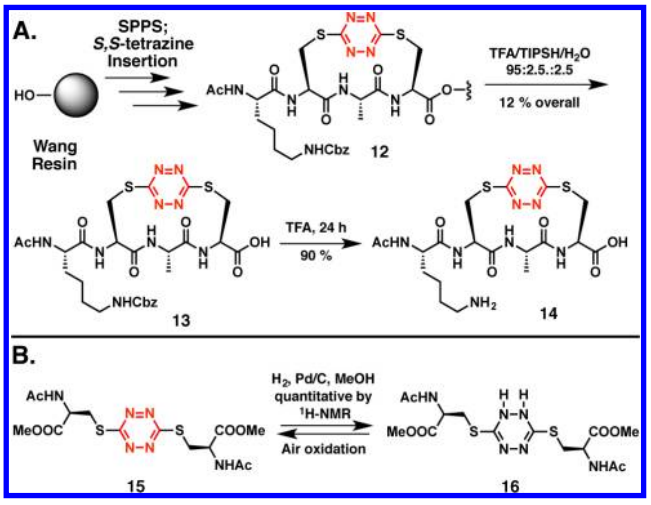

dx.doi.org/10.1021/jo402680v | J. Org. Chem. 2014, 79, 759−768

distinguish the tautomer obtained upon semihydrogenation, density functional theory (DFT) calculations at the RB3PW91/6-31+G(d,p) level were performed using Gaussian 09[37] to determine the frequencies and intensities of the IR transitions corresponding to the 1,2- and 1,4-dihydro-*S*,*S*-terazine tautomers. A correction factor based on the ratio of known experimental carbonyl frequencies to those derived from the DFT calculations was applied to the frequencies. The best agreement between the calculated and experimental infrared transitions suggested the formation of 1,2-dihydro-*S*,*S*-tetrazine **16**. Importantly, exposure of **16** to air over a 24 h period demonstrated that the dihydro-*S*,*S*-tetrazine **16** does indeed oxidize to give *S*,*S*-tetrazine **15**.

With the use of the Cbz protecting group validated, the synthesis of the target ***S*,*S*-Tet-AKA** peptide employing a three-fragment union tactic was undertaken (Scheme 6). The

Scheme 6. The Successful Three-Fragment Union Approach To Synthesize *S*,*S*-Tet-AKA

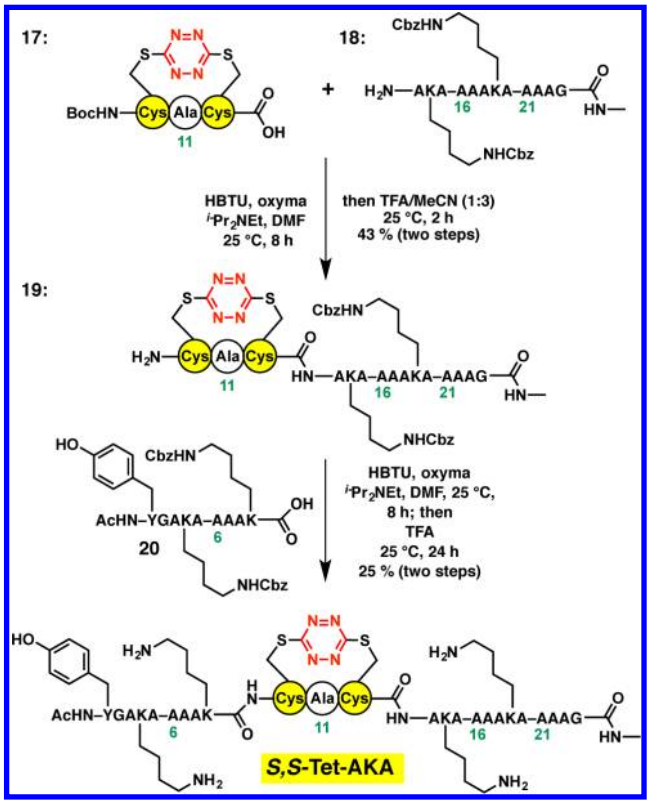

appropriate linchpin **17** was available from our model studies,[29] while the requisite *C*- and *N*-terminal peptide fragments **18** and **20** were constructed via SPPS employing the *N*-methylindole and 2-chlorotrityl resins, respectively. The free amine of peptide **18** was first coupled to *S*,*S*-tetrazine linchpin **27**, followed by the removal of the Boc protecting group, to furnish peptide **19** in 43% yield for the two steps. Peptide **19** in turn was coupled to the *N*-terminal peptide fragment **20**, followed by treatment with TFA, to complete the construction of the peptide ***S*,*S*-Tet-AKA**.[30] The final union and deprotection proceeded in 25% yield after HPLC purification.

Synthetic ***S*,*S*-Tet-AKA** was characterized by HPLC–MS and MALDI-TOF MS. Pleasingly, the far-UV CD spectra of ***S*,*S*-Tet-AKA** in TFE (Figure 3) indicated the fractional helicity to be 0.43, similar to that of the proline-kinked mutant $\mathbf{AKA}_{\mathbf{A11P}}$ model (vide supra). For the proposed transient 2D-IR experiments, this fractional helicity was required in order to observe conformational reorganization to the final α-helical structure upon photolysis of the *S*,*S*-tetrazine constraint.

Photochemical Studies: Kinetics and Conformational Response to Photorelease. The synthetic ***S*,*S*-Tet-AKA** peptide was first subjected to steady-state photolysis (λ = 355 nm) to afford the $\mathbf{(SCN)_2}$**-AKA** peptide (see Figure 1B) in TFE. We were delighted to find that the fractional helicity of $\mathbf{(SCN)_2}$**-AKA** was 0.50, representing roughly a 0.07 increase in the helical content upon release of the *S*,*S*-tetrazine photo-trigger. In view of the fact that only a single α-helix turn is formed following the *S*,*S*-tetrazine photolysis, the observed modest increase in helicity was expected. Transient 2D-IR measurements reported elsewhere[30] also confirmed the formation of the single α-helix turn following photolysis with a time constant of ~100 ps. To ensure that photolysis of the *S*,*S*-tetrazine linker was complete, formation of the SCN functionality was confirmed by FT-IR spectroscopy through observation of the SCN stretching band.[30]

The tripeptide model system **21**[29] (Figure 4 inset) was also employed to provide insights into the photochemistry of the

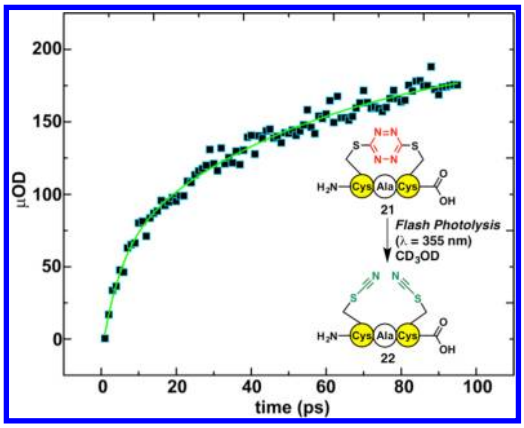

Figure 4. Time-dependent spectrum of the SCN transient absorption observed upon photolysis (355 nm excitation) of *S*,*S*-tetrazine tripeptide **21** to furnish bis-SCN tripeptide **22**, measured at 2163 cm^{-1} from 0 to 100 ps. The raw data points are black squares outlined in blue, while the exponential fit to data, with a time constant τ = 56 ps, is shown by the green curve.

kinked region. Upon photolysis of **21**, the yield of **22** measured by nanosecond transient absorption was 28%, slightly larger than the 20% previously observed for the photolysis of noncyclic *S*,*S*-tetrazine peptide **15**.[28] The increase in photochemical yield is likely related to the conformational strain exerted on the *S*,*S*-tetrazine system when the Cys residues are in an *i*, *i* + 2 relationship within cyclic peptide **21**. The time scale of SCN formation upon flash photolysis of **21** was determined by femtosecond transient spectroscopy[27,28] by measuring the time dependence of the increase of the SCN absorption band intensity of the peptide photoproduct **22** centered at 2163 cm^{-1} (Figure 4). The time constant for SCN formation was determined to be ~56 ps, again slightly shorter than that previously reported for the acyclic system **15**. On the basis of these experiments, the time required for formation of the final photoproduct **22** is expected to be on the order of tens of picoseconds, while the initial time scale for *S*,*S*-tetrazine ring cleavage of acyclic **15** was determined by prior experiments to be ~10 ps.[28]

dx.doi.org/10.1021/jo402680v | *J. Org. Chem.* 2014, 79, 759–768

To monitor the picosecond structural transitions within the amide backbone by 2D-IR upon photochemical release of ***S,S*-Tet-AKA**, the amide-I stretching modes were differentiated by employing carbonyl isotopic editing. Specifically, we incorporated the $^{13}C{=}^{18}O$ double label at defined positions along the peptide backbone.[38−42] Our modular fragment coupling strategy was well-suited to prepare these peptides, as we had previously reported a $^{13}C{=}^{18}O$ isotopically edited *S,S*-tetrazine linchpin[29] that we utilized here to prepare labeled peptide ***S,S*-Tet-AKA$_{C10*/A11*}$** (Figure 5). In addition, to monitor the backbone dynamics distal to the *S,S*-tetrazine phototrigger, two adjacent units of $^{13}C{=}^{18}O$-Ala[43] were incorporated within two *S,S*-tetrazine peptides, the first pair within the *N*-terminal peptide fragment, leading to the synthesis of ***S,S*-Tet-AKA$_{A5*/A6*}$**, and the second pair within the *C*-terminal peptide fragment, furnishing ***S,S*-Tet-AKA$_{A17*/A18*}$**. Standard SPPS utilizing $^{13}C{=}^{18}O$-Ala at the requisite positions, followed by the fragment union tactic, was employed.

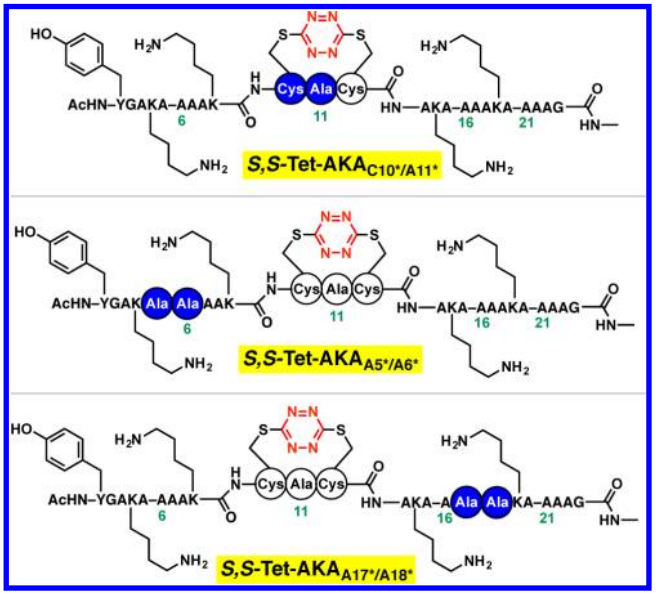

Figure 5. Isotopically edited peptides ***S,S*-Tet-AKA$_{C10*/A11*}$**, ***S,S*-Tet-AKA$_{A5*/A6*}$**, and ***S,S*-Tet-AKA$_{A17*/A18*}$** were synthesized to resolve the amide-I stretching modes from the remaining backbone stretching modes. The positions of the $^{13}C{=}^{18}O$-labeled amides in the synthetic peptides are shown as blue circles.

Upon evaluation of ***S,S*-Tet-AKA$_{A5*/A6*}$** and ***S,S*-Tet-AKA$_{A17*/A18*}$** by standard 2D-IR methods, the coupling between these dipoles indicated that the peptides have an α-helical structure in both the *N*- and *C*-terminal domains, respectively.[44,45] Subsequent evaluation of the *N*- or *C*-terminal-labeled residues by transient 2D-IR probe spectroscopy revealed no changes in the angle between the dipoles following *S,S*-tetrazine photolysis, suggesting that these regions of the peptide do not undergo conformational changes. As previously reported, only in the case of ***S,S*-Tet-AKA$_{C10*/A11*}$**, where the residues are in the domain of the peptide that is inscribed by the *S,S*-tetrazine constraint, did we observe significant changes in the conformation of the peptide.[30] Equally important and as described in detail elsewhere,[30] the ϕ and ψ angles could be extracted from the transient 2D IR spectra of the $^{13}C{=}^{18}O$ amides of Cys10 and Ala11 to reveal directly the rate of relaxation to the full helical structure. As the distal residues (cf. ***S,S*-Tet-AKA$_{A5*/A6*}$** and ***S,S*-Tet-AKA$_{A17*/A18*}$**) do not support conformational changes, we have proposed a model for this conformational transition wherein the dominant motion of the peptide is predominantly through rotation about the ψ dihedral angle.[30]

■ CONCLUSION

We report here the design and validation of a general synthetic protocol that permits incorporation of the *S,S*-tetrazine photochemical trigger into complex peptides. Photochemical release and monitoring by 2D-IR spectroscopy permits atomic-level definition of the microscopic motions that specific peptide/protein structural components explore along conformational reorganization paths to reach a final equilibrium structure. The specific photochemical trigger, *S,S*-tetrazine, was introduced into the alanine-rich α-helical AKA peptide to disrupt the extended helical conformation, similar to a helix−"proline turn"−helix. The bias to assume an extended α-helix conformation, however, initially hindered efforts to incorporate the *S,S*-tetrazine phototrigger directly employing our previously developed protocols. To overcome this challenge, the separate peptide fragments were constructed through SPPS, and a fragment union tactic was executed in solution to furnish the relatively large 24-residue ***S,S*-Tet-AKA** peptide system, which pleasingly adopts a well-defined initial conformational distribution. The initial helix−turn−helix conformation with the minor *S,S*-tetrazine perturbation within the middle of the sequence permitted 2D-IR observation of the microscopic structural transitions following ultrafast photochemical release. A detailed account of the conformational dynamics observed for the ***S,S*-Tet-AKA** peptide is now available.[30] Pleasingly, the synthetic methods developed herein hold the promise of wide applicability for the construction of diverse peptides and proteins possessing the ultrafast photochemical trigger *S,S*-tetrazine to define the early events in peptide/protein conformation reorganization.

■ EXPERIMENTAL SECTION

General Experimental Methods. Organic solvents used for reactions and washes were of reagent grade and degassed by purging with nitrogen prior to use. Di-*tert*-butyl dicarbonate (Boc_2O), diisopropylethylamine (DIPEA), acetic anhydride, *N*-methylimidazole, *O*-(benzotriazol-1-yl)-*N,N,N′,N′*-tetramethyluronium (HBTU), 1-(mesitylene-2-sulfonyl)-3-nitro-1*H*-1,2,4-triazole (MSNT), ethyl 2-cyano-2-(hydroxyimino)acetate (oxyma), Fmoc-Ala-OH, Fmoc-Cys-(Mmt), Fmoc-Asp(O*t*-Bu)-OH, Fmoc-Gly-OH, Fmoc-Pro-OH, Fmoc-Ser-OH, Fmoc-Trp(*N*-Boc)-OH, Fmoc-Val-OH, Fmoc-Ala-OH (1-^{13}C), L-cysteine (1-^{13}C), and ^{18}O water were purchased from commercial vendors and used as received. Wang resin (LL) and *N*-methylindole aminomethyl resins for peptide synthesis were obtained from Novabiochem.

Solid-phase syntheses were carried out in peptide synthesis reaction vessels (25 or 50 mL) with coarse-porosity fritted glass supports and Teflon stopcocks. The reaction vessels had 14/20 ground glass joints that allowed the resin to be kept under a nitrogen atmosphere while removing the monomethoxytrityl groups from cysteine. Photolysis experiments were performed in a Srinivasan−Griffin photoreactor. Microwave irradiation was employed using 2−5 mL sealed microwave reaction vessels, and an IR temperature sensor was used to control the temperature.

A chloranil test was used to examine the presence of free amines on resin. A test tube containing a small amount of resin (10−12 beads) known to have a free primary amine was used as a reference along with another test tube containing a small amount of the same resin after acylation. Each resin was first washed with DMF (3 × 1 mL) and then to each in DMF (1 mL) was added 1 drop of 2% (w/w) acetaldehyde/

dx.doi.org/10.1021/jo402680v | J. Org. Chem. 2014, 79, 759−768

DMF, immediately followed by 1 drop of 2% (w/w) 2,3,5,6-tetrachloro-1,4-benzoquinone (*p*-chloranil)/DMF and allowed to stand at room temperature for 5 min. The reaction solution was then removed by syringe and washed with DMF. The free amine resin (control) turned a deep-blue color while the acylated resin remained unchanged, suggesting that the amine had been completely acylated. The alizarin−cyanuric chloride test was used to test for alcohols on resin. Two resins in separate test tubes, one Wang resin and the other acylated Wang resin, were used. Each was washed with DMF (3 × 1 mL), and then a cocktail of *N*-methylmorpholine (1 mL), cyanuric chloride (5 mg), and DMF (3 mL) was added to each tube and heated at 70 °C for 20 min. The resin beads were washed with DMF (3 × 1 mL). Next, a solution of *N*-methylmorpholine (1 mL), alizarin (5 mg), and DMF (3 mL) was added, and after 5 min the resin beads were washed with DMF. The Wang resin turned dark red, while the acylated resin remained colorless.

Resin washing was conducted with the indicated solvent and was allowed to contact the resin for 30 s during each wash. The solvent was pushed through the frit using an "air push" apparatus made from a 15 mL disposable syringe and a 14/20 septum, or nitrogen gas was used in cases of an inert atmosphere requirement.

Preparative-scale reversed-phase chromatography was conducted using binary HPLC pumps and a UV−vis dual-wavelength detector. The separations were achieved with a Waters XBridge Prep BEH 130 C18 5 μm OBD 19 mm × 100 mm column. The eluent was acetonitrile (HPLC grade) and Millipore water with 0.05% formic acid buffer, unless otherwise noted. Linear gradient elutions with a flow rate of 15 mL/min were employed, and specific gradients for each compound are noted.

^{1}H NMR (500 MHz), ^{13}C NMR (125 MHz), and 2D NMR spectra were recorded with either a 5 mm dual inverse probe or a 5 mm DCH CryoProbe. Analytical LC−MS analyses were conducted on a binary gradient HPLC system connected to a diode array detector and a mass spectrometer with electrospray ionization. The HPLC−MS samples were analyzed as solutions in water or acetonitrile, prepared at 0.15−0.20 mg/mL concentration. The analytical HPLC−MS analyses were conducted with an Atlantis C18 column (4.6 mm × 50 mm; 5 μm), and linear gradients of 0.05% formic acid in acetonitrile and 0.05% formic acid water were utilized with a flow rate of 2 mL/min. High-resolution mass spectrometry (HRMS) was performed with a MALDI-TOF-TOF mass spectrometer using electrospray ionization in positive or negative mode, depending upon the analyte. All FTIR spectra were obtained using default parameters. Absorption spectra were taken with a UV−vis spectrometer, and CD spectra were obtained with a 1 mm sample holder.

Femtosecond IR Transient Absorption Method. The optical density (OD) of the samples at the excitation wavelength (355 nm) ranged from 0.09 to 0.12 in a 400 μm path length CaF_2 cell for femtosecond transient IR experiments. Fourier transform-limited 70 fs pulses with center frequencies of 2150 cm^{-1} were used in the femtosecond IR transient absorption experiments for the samples in chloroform. The energy of the 355 nm excitation pulse (5 μJ) was attenuated by an iris. The beam radius of the IR probe pulse was 75% of the visible pump pulse radius at the sample cell. The beam radius of the IR probe pulse was 75% of the visible pump pulse radius at the sample cell. The visible beam was passed through a hole in the center of the parabolas used to collect the infrared probe pulses, and the overlap between the pump and probe pulses was achieved by first using a 200 μm pinhole at the sample holder and then maximizing the transient absorption signal of a Si wafer. The transient absorption of the carbonyl stretch of fluorenone was utilized as a standard to optimize the overlap of the pump beam. The timing between the pump and probe pulses was varied by using an automated translation stage with femtosecond time resolution. The transmitted probe pulse was focused onto the focal plane of a monochromator equipped with a 64-element mercury−cadmium−telluride array detector. The appropriate monochromator grating was chosen, comprising 150 lines per mm groove. The kinetic trace was collected (averaged over 16 scans, 1600 shots per scan) over a 100 ps time range with 1 ps steps.

General Resin Loading Procedures. *Wang Resin.* The resin (0.22 mmol) was placed in a peptide synthesis vessel and swelled with CH_2Cl_2 (10 mL) for 1 h. The solvent was drained, and a premixed solution of Fmoc-AA-OH (0.88 mmol, 4.0 equiv), MSNT (0.88 mmol, 4.0 equiv), and methylimidazole (0.66 mmol, 3.0 equiv) dissolved in CH_2Cl_2 (5 mL) was added to the resin. The contents were gently rocked for 2 h and then drained, and the resin was washed with CH_2Cl_2 (3 × 5 mL). The procedure was repeated and the resin carried on to the next step.

N-Methylindole AM Resin. *N*-Methylindole resin (0.22 mmol) was placed in a peptide synthesis vessel and swelled with CH_2Cl_2 (10 mL) for 1 h. The solvent was drained, and the resin was then treated with a solution of 20% piperidine/DMF (2 × 7 mL), allowing each treatment to contact the resin for 10 min. The resin was then washed with DMF (3 × 5 mL), and a premixed solution of Fmoc-AA-OH (1.1 mmol, 5 equiv), HBTU (1.1 mmol, 5 equiv), oxyma (1.1 mmol, 5 equiv), and DIPEA (2.2 mmol, 10 equiv) dissolved in DMF (5 mL) was added to the resin. The contents were rocked gently for 1 h and then drained, and the resin was washed with DMF (3 × 5 mL). The coupling procedure was repeated and the resin carried on to the next step.

2-Chlorotrityl Chloride Resin. 2-Chlorotrityl chloride resin (0.22 mmol) was placed in a peptide synthesis vessel and swelled with CH_2Cl_2 (10 mL) for 1 h. The solvent was drained, and then a premixed solution of Fmoc-AA-OH (0.26 mmol, 1.2 equiv) and DIPEA (0.88 mmol, 4 equiv) dissolved in CH_2Cl_2 (5 mL) was added to the resin. The contents were rocked gently for 1 h and then drained, and the resin was washed with DMF (3 × 5 mL). The coupling procedure was repeated and the resin carried on to the next step.

General Procedures for Solid-Phase Peptide Synthesis. The resin-bound Fmoc-amino acid (0.22 mmol) was washed with DMF (3 × 5 mL) and then treated with a 20% piperidine/DMF solution (2 × 7 mL), allowing each treatment to contact the resin for 10 min. The resin was washed with DMF (3 × 5 mL), and then a premixed solution of Fmoc-protected amino acid (1.1 mmol, 5.0 equiv), HBTU (1.1 mmol, 5.0 equiv), oxyma (1.1 mmol, 5.0 equiv), and DIPEA (2.2 mmol, 10.0 equiv) dissolved in DMF (5 mL) was added to the resin. The contents were rocked gently for 1 h and then drained, and the resin was washed with DMF (3 × 5 mL). The Fmoc deprotection procedure was repeated, followed by the coupling of the amino acid sequence to synthesize the desired peptide. The *N*-terminus was protected as the Boc- or Ac-derivative by first employing the Fmoc deprotection procedure and washing the resin with DMF (3 × 5 mL). A premixed solution of Boc-anhydride (2.2 mmol, 10 equiv)/acetic anhydride (2.2 mmol, 10 equiv) and DIPEA (4.4 mmol, 20 equiv) in DMF (5 mL) was added to the resin. The contents were rocked gently for 1 h and then drained, and the resin was sequentially washed with DMF (3 × 5 mL) and CH_2Cl_2 (3 × 5 mL).

***S,S*-Tetrazine Tethering during SPPS.** The resin-bound peptide (0.22 mmol) containing two *S*-Mmt-protected Cys groups was swelled with CH_2Cl_2 (10 mL) for 1 h. The peptide synthesis vessel was then sealed with a septum, vented to a mineral-oil-filled bubbler, and attached to a two-neck collection flask. The solvent was drained, and a premixed solution of CH_2Cl_2/TIPSH/TFA (92.5:5.0:2.5 peptides on the Wang resin; 95:4:1 for loaded *N*-methylindole AM resin) was added to the resin, after which a stream of nitrogen was introduced through the collection flask and bubbled through the resin bed to agitate the orange reaction mixture for 3 min. The contents were drained by pushing the liquid contents into the collection flask using a stream of nitrogen, and the resin was washed with CH_2Cl_2 (10 mL). The procedure was repeated four additional times until the reaction solution became clear, suggesting that the monomethoxytrityl groups had been completely removed. The resin was washed with 10% DIPEA/$ClCH_2CH_2Cl$ (3 × 5 mL). To the resin was added a solution of dichlorotetrazine (**2**) (0.24 mmol, 1.1 equiv) in $ClCH_2CH_2Cl$ (5 mL) followed by neat DIPEA (0.5 mL). The peptide vessel was wrapped in foil to exclude ambient light, and the contents were agitated for 18 h. The solvent was drained, and the resin was washed with CH_2Cl_2 (3 × 5 mL), MeOH (3 × 5 mL), and CH_2Cl_2 (3 × 5 mL).

dx.doi.org/10.1021/jo402680v | *J. Org. Chem.* 2014, 79, 759−768

Synthesis and Isolation of Peptides. ***AKA*** *Peptide.* This previously reported peptide[31] was prepared from 0.050 mmol of loaded methylindole AM resin following the general procedures. The final product was purified by reversed-phase HPLC (gradient 5−35% organic over 10 min) to give 13.7 mg (13% yield) of a white amorphous powder after lyophilization. HRMS (ES) *m*/*z* 2093.1575 [(M + Na)$^+$; calcd for $C_{91}H_{155}N_{29}O_{26}Na$, 2093.1596]; MALDI-TOF *m*/*z* 2071.014 [(M + H)$^+$; calcd for $C_{92}H_{156}N_{29}O_{26}$, 2071.1776].

AKA$_{A11P}$ *Peptide.* The **AKA$_{A11P}$** peptide was prepared from 0.050 mmol of loaded methylindole AM resin utilizing the general procedures and purified by reversed-phase chromatography (gradient 5−35% organic over 10 min) to afford 27.8 mg (27% yield) of **AKA$_{A11P}$** as a white amorphous powder after lyophilization. HRMS (ES) *m*/*z* 2097.1933 [(M + H)$^+$; calcd for $C_{93}H_{158}N_{29}O_{26}$, 2097.1980]; MALDI-TOF *m*/*z* 2097.123 [(M + H)$^+$; calcd for $C_{93}H_{158}N_{29}O_{26}$, 2097.1980].

AKA$_{A10C/A12C}$ *Peptide.* The **AKA$_{A10C/A12C}$** peptide was prepared from 0.036 mmol of loaded methylindole AM resin employing the general procedures and purified by reversed-phase chromatography (gradient 5−35% organic over 10 min) to give 10.5 mg (15% yield) of **AKA$_{A10C/A12C}$** as a white amorphous powder after lyophilization. HRMS (ES) *m*/*z* 2157.1082 [(M + Na)$^+$; calcd for $C_{91}H_{155}N_{29}O_{26}NaS_2$, 2157.1037]; MALDI-TOF *m*/*z* 2157.315 [(M + Na)$^+$; calcd for $C_{91}H_{155}N_{29}O_{26}NaS_2$, 2157.1037].

S,S-Tetrazine Tetrapeptide ***3***. Tetrapeptide **3** was synthesized from 0.22 mmol of loaded methylindole AM resin employing the general procedures and purified by reversed-phase chromatography (gradient 5−45% organic over 12 min) to give 12.2 mg (10% yield) of **3** as an orange amorphous powder after lyophilization. All of the resonances for **3** were assigned using 2D NMR (COSY, HMBC, and HSQC): ^{1}H NMR (500 MHz, DMSO-d_6) δ 8.49 (d, Ala-3-NH, J = 8.5 Hz, 1H), 8.48 (d, Cys-4-NH, J = 7.0 Hz, 1H), 8.19 (d, Lys-1-NH, J = 8.0 Hz, 1H), 8.01 (q, Me-NH, J = 4.5 Hz, 1H), 7.84 (d, Cys-2-NH, J = 6.5 Hz, 1H), 4.71 (dt, Cys-2-Hα, J = 6.5, 3.5 Hz, 1H), 4.68 (ddd, Cys-4-Hα, J = 6.5, 4.5, 2.0 Hz, 1H), 4.50 (dd, Cys-4-Hβ, J = 15.0, 4.5 Hz, 1H), 4.46 (dd, Cys-2-Hβ, J = 15.0, 2.5 Hz, 1H), 4.26 (dq, Lys-1-Hα, J = 8.0, 4.5 Hz, 1H), 4.14 (dq, Ala-3-Hα, J = 8.5, 7.0 Hz, 1H), 3.45 (dd, Cys-4-Hβ, J = 14.5, 2.0 Hz, 1H), 3.34 (dd, Cys-2-Hβ, J = 14.5, 4.0 Hz, 1H), 2.76 (t, −CH_2−NH$_2$, J = 7.5 Hz, 2H), 2.64 (d, CH_3−NH, J = 4.5 Hz, 3H), 1.88 (s, CH_3−CO, 3H), 1.54−1.47 (m, 4H), 1.36−1.28 (m, 2H), 1.04 (d, Ala-3-CH$_3$, J = 7.0 Hz, 3H); ^{13}C NMR (125 MHz, DMSO-d_6) δ 171.4, 171.2, 170.3, 169.6, 168.9, 166.9, 52.5, 51.3, 51.0, 47.6, 38.8, 32.4, 31.1, 30.3, 26.7, 26.0, 22.6, 22.5, 19.8; HRMS (ES) *m*/*z* 557.2072 [(M + H)$^+$; calcd for $C_{20}H_{33}N_{10}O_5S_2$, 557.2077].

Steady-State Photolysis of Tetrapeptide ***3***. A solution of **3** in CD_3OD (~5 mg/mL) was photolyzed under steady-state irradition for 4 h to afford bis-SCN peptide **4**. ^{1}H NMR (500 MHz, CD_3OD) δ 4.72 (dd, J = 8.5, 4.5 Hz, 1H), 4.66 (dd, J = 7.5, 5.0 Hz, 1H), 4.34 (q, J = 7.0 Hz, 1H), 4.30 (dd, J = 8.0, 5.5 Hz, 1H), 3.64 (dd, J = 14.0, 4.5 Hz, 1H), 3.54 (dd, J = 14.0, 5.0 Hz, 1H), 3.37 (dd, J = 14.0, 9.0 Hz, 1H), 3.36 (dd, J = 14.0, 7.5 Hz, 1H), 2.99−2.94 (m, 2H), 2.77 (br s, 3H), 2.05−2.01 (overlapping m, 2H), 2.04 (overlapping s, 3H), 1.73−1.68 (m, 2H), 1.44 (d, J = 7.0 Hz, 3H); ^{13}C NMR (125 MHz, DMSO-d_6) δ 172.7, 172.5, 170.3, 169.1, 169.0, 113.6, 113.5, 53.3, 52.8, 52.7, 49.5, 39.14, 35.6, 31.5, 27.1, 26.3, 23.0, 22.8, 18.8; HRMS (ES) *m*/*z* 529.2007 [(M + H)$^+$; calcd for $C_{20}H_{33}N_8O_5S_2$, 529.2015].

S,S-Tetrazine Peptide ***8***. Peptide **8** was prepared from 0.13 mmol of loaded Wang resin employing the general procedures and purified by reversed-phase chromatography (gradient 5−30% organic over 12 min) to give 17.8 mg (20% yield) of **8** as an orange amorphous powder after lyophilization. HRMS (ES) *m*/*z* 686.2522 [(M + H)$^+$; calcd for $C_{25}H_{40}N_{11}O_8S_2$, 686.2503].

Peptide ***9***. A 25 mL round-bottom flask was charged with **8** (6.0 mg, 0.0088 mmol) and $NaHCO_3$ (1.8 mg, 0.022 mmol, 2.5 equiv), which were then dissolved in water (2.0 mL). A premixed solution of Boc_2O (2.9 mg, 0.013 mmol, 1.5 equiv) dissolved in 1,4-dioxane (1.0 mL) was added, and the reaction solution was heated to 45 °C with stirring. After 30 min, completion of the reaction was observed by LC−MS, and the reaction solution was directly purified by reversed-phase chromatography (gradient 5−50% organic over 10 min) to give 5.5 mg (80% yield) of **9** as a red-orange amorphous powder after lyophilization. HRMS (ES) *m*/*z* 808.2853 [(M + Na)$^+$; calcd for $C_{30}H_{47}N_{11}O_{10}NaS_2$, 808.2847].

Peptide Building Block ***10***. The peptide sequence comprising the *N*-terminal fragment of the target peptide was assembled from 0.10 mmol of loaded methylindole AM resin employing the general procedures, cleaved from the resin to retain the *N*-terminal Fmoc protecting group, and purified by reversed-phase chromatography (gradient 5−35% organic over 10 min) to give 65.4 mg (54% yield) of **10** as a white amorphous powder after lyophilization. HRMS (ES) *m*/*z* 1206.6654 [(M + H)$^+$; calcd for $C_{57}H_{88}N_{15}O_{14}$, 1206.6635]. Next, to install the requisite *N*(ε)-Boc protecting groups, a 25 mL round-bottom flask was charged with the above peptide (30.0 mg, 0.025 mmol) and $NaHCO_3$ (10.5 mg, 0.125 mmol, 5 equiv), which were then dissolved in water (2.0 mL). A premixed solution of Boc_2O (16.4 mg, 0.075 mmol, 3 equiv) dissolved in 1,4-dioxane (2.0 mL) was added, and the reaction solution was heated to 45 °C with stirring. After 2 h, completion of the reaction was observed by LC−MS, and the solvent was evaporated under reduced pressure. The crude reaction mixture was dissolved in DMF (2.0 mL), and then added dropwise by syringe with stirring to a 25 mL round-bottom flask charged with 10% piperidine/DMF (2.0 mL). Once the addition was completed, the reaction solution was allowed to stir at room temperature for 10 min and then concentrated under reduced pressure. The resulting residue was dissolved in 1:1 acetonitrile/water and then purified by reversed-phase chromatography (gradient 5−60% organic over 10 min) to give 19.8 mg (67% yield) of **10** as an amorphous powder after lyophilization. HRMS (ES) *m*/*z* 1184.6713 [(M + H)$^+$; calcd for $C_{52}H_{94}N_{15}O_{16}$, 1184.6998].

Peptide ***11***. To a 10 mL teardrop flask containing peptide **10** (3.3 mg, 0.0028 mmol) in DMF (1 mL) was added dropwise a premixed solution of **9** (4.4 mg, 0.0056 mmol, 2.0 equiv), oxyma (0.80 mg, 0.0056 mmol, 2.0 equiv), HBTU (2.1 mg, 0.0056 mmol, 2.0 equiv), and DIPEA (2.3 μL, 0.014 mmol, 5 equiv) in DMF (1.0 mL). After 3 h of stirring, completion of the reaction was observed by LC−MS, and the solution was concentrated under reduced pressure. The resulting residue was taken into 1:1 acetonitrile/water and then purified by reversed-phase chromatography (gradient 5−70% organic over 10 min) to give 2.9 mg (53% yield) of the protected peptide intermediate as a light-orange amorphous powder after lyophilization. HRMS (ES) *m*/*z* 1973.9673 [(M + Na)$^+$; calcd for $C_{82}H_{38}N_{26}O_{25}NaS_2$, 1973.9666]; MALDI-TOF *m*/*z* 1973.761 [(M + Na)$^+$; calcd for $C_{82}H_{38}N_{26}O_{25}NaS_2$, 1973.9666]. Next, a 10 mL teardrop flask charged with the protected peptide intermediate (2.9 mg, 0.0015 mmol) and a solution of 1:3 TFA/CH_3CN (2 mL) was added in one portion. After 2 h of stirring, completion of the reaction was observed by LC−MS, and the solution was concentrated under reduced pressure to afford, without any purification, 2.5 mg of peptide **11** as a light-orange amorphous powder. HRMS (ES) *m*/*z* 1651.8291 [(M + H)$^+$; calcd for $C_{67}H_{114}N_{26}O_{19}S_2$, 1651.8273]; MALDI-TOF *m*/*z* 1651.355 [(M + H)$^+$; calcd for $C_{67}H_{114}N_{26}O_{19}S_2$, 1651.8273].

S,S-Tetrazine Tetrapeptide ***13***. The Cbz-protected peptide **13** was synthesized from 0.11 mmol of loaded Wang resin employing the general procedures and purified by reversed-phase chromatography (gradient 10−80% organic over 10 min) to give 11.9 mg (16% yield) of an orange amorphous powder after lyophilization. HRMS (ES) *m*/*z* 700.1962 [(M + Na)$^+$; calcd for $C_{27}H_{35}N_9O_8NaS_2$, 700.1948]. The ^{1}H NMR spectrum (DMSO-d_6) indicated the presence of the diagnostic β-Cys resonances for peptides contining the *S,S*-tetrazine phototrigger; however, multiple conformers were observed for this protected peptide intermediate (see the Supporting Information).

S,S-Tetrazine Peptide ***14***. To a 10 mL teardrop flask charged with **13** (2.0 mg, 0.0030 mmol) was added a solution of 19:1 TFA/TIPSH (3 mL). After 2 h of stirring, completion of the reaction was observed by LC−MS, and the solution was concentrated under reduced pressure. The resulting residue was taken into water (1 mL) and then purified by reversed-phase chromatography (gradient 5%−45% organic over 10 min) to give 1.5 mg (90% yield) of **14** as an orange amorphous powder after lyophilization. ^{1}H NMR (500 MHz, DMSO-d_6) δ 8.44 (d, J = 6.5 Hz, 1H), 8.48 (d, J = 8.5 Hz, 1H), 8.18 (d, J = 8.0

dx.doi.org/10.1021/jo402680v | *J. Org. Chem.* 2014, 79, 759−768

Hz, 1H), 7.83 (d, J = 7 Hz, 1H), 7.74 (br s, 1H), 6.51 (s, 2H), 4.79 (br m, 1H), 4.74 (dt, J = 6.5, 3.5 Hz, 1H), 4.54 (m, 2H), 4.25 (ddd, J = 8.6, 4.8, 3.5 Hz, 1H), 4.17 (ddd, J = 7.6, 6.4, 1.0 Hz, 1H), 3.52 (dd, J = 14.9, 1.8 Hz, 1H), 3.37 (dd, J = 15.2, 3.5 Hz, 1H), 2.76 (br m, 2H), 1.88 (s, 3H), 1.63 (br m, 1H), 1.52 (br m, 4H), 1.37−1.31 (br m, 3H), 1.00 (d, J = 6.5 Hz, 3H); ^{13}C NMR (125 MHz, DMSO-d_6) δ 171.1, 170.8, 170.6, 170.4, 169.4, 166.8, 52.4, 51.6, 50.9, 47.4, 38.6, 32.3, 30.9, 30.3, 26.6, 22.5, 22.3, 19.7 (note: one peak overlapped with the solvent signal); HRMS (ES) m/z 544.1777 [(M + H)$^+$; calcd for $C_{19}H_{30}N_9O_6S_2$, 544.1760].

Dihydro-S,S-tetrazine ***16***. A 10 mL teardrop flask equipped with a stir bar was charged with a solution of **15**[27] (15.0 mg, 0.035 mmol) in methanol (5 mL). A spatula tip of 10% palladium on carbon (50% wet with water) was added to the solution. The heterogeneous mixture was flushed with hydrogen gas using a balloon and then stirred under a hydrogen gas environment for 5 min. The mixture was then filtered through a pad of silica gel, and the filterate was concentrated in vacuo to afford, without any required purification, 14.9 mg (98% yield) of **16** as a colorless oil. IR (CH_2Cl_2) 3047 (s), 2985 (s), 2306 (m), 1745 (s), 1679 (s), 1623 (m), 1510 (s) cm^{-1}; ^{1}H NMR (500 MHz, CD_3OD) δ 4.69 (dd, J = 8.0, 4.5 Hz, 1H), 3.73 (s, 3H), 3.46 (dd, J = 14.0, 4.5 Hz, 1H), 3.22 (dd, J = 14.0, 8.0 Hz, 1H), 1.99 (s, 3H); ^{1}H NMR (500 MHz, DMSO-d_6) δ 8.89 (s, 1H), 4.43 (d, J = 7.5 Hz, 1H), 4.89 (ddd, J = 9.0, 7.5, 5.0 Hz, 1H), 3.63 (s, 3H), 3.33 (dd, J = 13.5, 5.0 Hz, 1H), 3.06 (dd, J = 13.5, 9.0 Hz, 1H), 1.86 (s, 3H); ^{13}C NMR (125 MHz, CD_3OD) δ 173.5, 172.3, 151.8, 54.0, 53.2, 33.2, 22.5; ^{13}C NMR (125 MHz, DMSO-d_6) δ 170.7, 169.3, 149.4, 52.1, 51.5, 31.2, 22.2; HRMS (ES) m/z 435.1129 [(M + H)$^+$; calcd for $C_{14}H_{23}N_6O_6S_2$, 435.1121].

To a 10 mL teardrop flask charged with **16** (5.2 mg, 0.012 mmol) was added methanol (5 mL). The solution was allowed to stand exposed to air for 8 h, after which the solution, which turned from colorless to orange, was concentrated in vacuo and then chromatographed on silica gel using 5% methanol/ethyl acetate as the eluent to give 5.0 mg (97% yield) of **15** as an orange solid. The characterization data for this material matched that reported previously for **15**.[27] To provide evidence as to whether **16** was the 1,2- or 1,4-dihydrotetrazine, IR analysis aided with simulations were highly suggestive of the 1,2-dihydrotetrazine (see the Supporting Information).

Peptide ***18***. Peptide **18**, comprising the *C*-terminal fragment of ***S,S*-Tet-AKA**, was synthesized from 0.25 mmol of loaded methylindole AM resin according to the general procedures and purified by reversed-phase chromatography (gradient 5−60% organic over 10 min) to provide 116.1 mg (37% yield) of **18** as a white amorphous powder after lyophilization. HRMS (ES) m/z 1252.6707 [(M + H)$^+$; calcd for $C_{58}H_{90}N_{15}O_{16}$, 1252.6690]; MALDI-TOF m/z 1274.399 [(M + Na)$^+$; calcd for $C_{58}H_{89}N_{15}O_{16}Na$, 1274.6510].

Peptide ***19***. To a 25 mL teardrop flask containing peptide **18** (53.0 mg, 0.043 mmol) in DMF (3.5 mL) was added dropwise a premixed solution of **17**[29] (20.0 mg, 0.043 mmol, 1.0 equiv), oxyma (6.7 mg, 0.047 mmol, 1.1 equiv), HBTU (17.9 mg, 0.047 mmol, 1.1 equiv), and DIPEA (18.7 μL, 0.11 mmol, 2.5 equiv) in DMF (1.5 mL). After 8 h of stirring, the reaction solution was concentrated under reduced pressure. To the resulting residue was added a 1:3 TFA/CH_3CN solution (5 mL). After 2 h of stirring, the reaction solution was directly purified by reversed-phase chromatography (gradient 10−70% organic over 10 min) to give 32.8 mg (43% yield) of **19** as an amorphous powder after lyophilization. HRMS (ES) m/z 1629.7113 [(M + Na)$^+$; calcd for $C_{69}H_{102}N_{22}O_{19}NaS_2$, 1629.7031]; MALDI-TOF m/z 1629.665 [(M + Na)$^+$; calcd for $C_{69}H_{102}N_{22}O_{19}NaS_2$, 1629.7031].

Peptide ***20***. Peptide **20**, comprising the *N*-terminal fragment of ***S,S*-Tet-AKA**, was prepared from 0.25 mmol of loaded 2-chlorotrityl chloride resin following the general procedures and purified by reversed-phase chromatography (gradient 10−70% organic over 10 min) to afford 109.1 mg (38% yield) of **20** as a white amorphous powder after lyophilization. HRMS (ES) m/z 1160.5630 [(M + H)$^+$; calcd for $C_{56}H_{78}N_{11}O_{16}$, 1160.5628]; MALDI-TOF m/z 1182.469 [(M + Na)$^+$; calcd for $C_{56}H_{77}N_{11}O_{16}Na$, 1182.5448].

Peptide ***S,S-Tet-AKA***. To a 10 mL teardrop flask containing peptide **19** (30.8 mg, 0.019 mmol) in DMF (2.5 mL) was added dropwise a premixed solution of **20** (22.3 mg, 0.019 mmol, 1.0 equiv), oxyma (3.0 mg, 0.021 mmol, 1.1 equiv), HBTU (8.0 mg, 0.021 mmol, 1.1 equiv), and DIPEA (8.4 μL, 0.048 mmol, 2.5 equiv) in DMF (1.5 mL). After 8 h of stirring, the reaction solution was concentrated under reduced pressure. To the resulting residue was added neat TFA (4 mL). After 24 h of stirring, the solution was concentrated under reduced pressure, taken into 1:1 acetonitrile/water, and then purified by reversed-phase chromatography (gradient 5−35% organic over 10 min; the formic acid buffer for the mobile phase was replaced with 0.05% TFA) to provide 10.5 mg (25% yield) of ***S,S*-Tet-AKA** as an amorphous powder after lyophilization. HRMS (ES) m/z 2213.1260 [(M + H)$^+$; calcd for $C_{93}H_{154}N_{33}O_{26}S_2$, 2213.1184]; MALDI-TOF m/z 2213.598 [(M + H)$^+$; calcd for $C_{93}H_{154}N_{33}O_{26}S_2$, 2213.1184].

Isotopically Edited Peptides Containing ^{13}C/^{18}O Amides. The procedures described above were employed to synthesize the ***S,S*-Tet-AKA$_{C10*/A11*}$**, ***S,S*-Tet-AKA$_{A5*/A6*}$**, and ***S,S*-Tet-AKA$_{A17*/A18*}$** peptides utilizing either Fmoc-HN-Cys(*S*^{t}Bu)-$^{13}C^{18}O_2H$ or Fmoc-HN-Ala-$^{13}C^{18}O_2H$, which were prepared according to previously reported methods.[29,43] Mass spectra and LC−MS chromatograms of the synthetic intermediates are provided in the Supporting Information.

Peptide ***S,S-Tet-AKA$_{C10*/A11*}$***. HRMS (ES) m/z 2219.1348 [(M + H)$^+$; calcd for $^{12}C_{91}{}^{13}C_2H_{154}N_{33}{}^{16}O_{24}{}^{18}O_2S_2$, 2219.1336]; MALDI-TOF m/z 2219.522 [(M + H)$^+$; calcd for $^{12}C_{91}{}^{13}C_2H_{154}N_{33}{}^{16}O_{24}{}^{18}O_2S_2$, 2219.1336].

Peptide ***S,S-Tet-AKA$_{A5*/A6*}$***. HRMS (ES) m/z 2219.1357 [(M + H)$^+$; calcd for $^{12}C_{91}{}^{13}C_2H_{154}N_{33}{}^{16}O_{24}{}^{18}O_2S_2$, 2219.1336]; MALDI-TOF m/z 2219.781 [(M + H)$^+$; calcd for $^{12}C_{91}{}^{13}C_2H_{154}N_{33}{}^{16}O_{24}{}^{18}O_2S_2$, 2219.1336].

Peptide ***S,S-Tet-AKA$_{A17*/A18*}$***. HRMS (ES) m/z 2219.1414 [(M + H)$^+$; calcd for $^{12}C_{91}{}^{13}C_2H_{154}N_{33}{}^{16}O_{24}{}^{18}O_2S_2$, 2219.1336]; MALDI-TOF m/z 2219.756 [(M + H)$^+$; calcd for $^{12}C_{91}{}^{13}C_2H_{154}N_{33}{}^{16}O_{24}{}^{18}O_2S_2$, 2219.1336].

■ ASSOCIATED CONTENT

Ⓢ Supporting Information

HPLC−MS and MALDI-TOF-TOF data, a description of the simulated IR spectra for dihydro-*S,S*-tetrazine **16**, characterization data for synthetic intermediates related to the ^{13}C/^{18}O isotopically labeled peptides, and NMR spectra. This material is available free of charge via the Internet at http://pubs.acs.org.

■ AUTHOR INFORMATION

Corresponding Author

*E-mail: smithab@sas.upenn.edu.

Present Address

†M.J.T.: Department of Chemistry, University of Nevada, Reno, NV 89557.

Notes

The authors declare no competing financial interest.

‡Robin M. Hochstrasser, Donner Professor of Physical Sciences at the University of Pennsylvania, passed away on February 27, 2013.

■ ACKNOWLEDGMENTS

Financial support was provided by the NIH (GM 12694) and an RLBL Facility Grant (NIH P41 RR 001348). The MALDI-TOF-TOF instrumentation was supported by NSF MRI-0820996. The authors also thank Drs. George Furst and Rakesh Kohli at the University of Pennsylvania for assistance in obtaining NMR and HRMS spectra, respectively.

■ REFERENCES

(1) McCammon, J. A.; Gelin, B. R.; Karplus, M. *Nature* **1977**, *267*, 585.

(2) Henzler-Wildman, K. A.; Lei, M.; Thai, V.; Kerns, S. J.; Karplus, M.; Kern, D. *Nature* **2007**, *450*, 913.

(3) Henzler-Wildman, K.; Kern, D. *Nature* **2007**, *450*, 964.
(4) Smock, R. G.; Gierasch, L. M. *Science* **2009**, *324*, 198.
(5) Kolano, C.; Helbing, J.; Bucher, G.; Sander, W.; Hamm, P. *J. Phys. Chem. B* **2007**, *111*, 11297.
(6) Frauenfelder, H.; Sligar, S. G.; Wolynes, P. G. *Science* **1991**, *254*, 1598.
(7) Brooks, C. L.; Gruebele, M.; Onuchic, J. N.; Wolynes, P. G. *Proc. Natl. Acad. Sci. U.S.A.* **1998**, *95*, 11037.
(8) Wolynes, P. G.; Eaton, W. A.; Fersht, A. R. *Proc. Natl. Acad. Sci. U.S.A.* **2012**, *109*, 17770.
(9) Sborgi, L.; Verma, A.; Sadqi, M.; Alba, E.; Muñoz, V. *Methods Mol. Biol.* **2013**, *932*, 205.
(10) Henzler-Wildman, K. A.; Thai, V.; Lei, M.; Ott, M.; Wolf-Watz, M.; Fenn, T.; Pozharski, E.; Wilson, M. A.; Petsko, G. A.; Karplus, M.; Hübner, C. G.; Kern, D. *Nature* **2007**, *450*, 838.
(11) Cammarata, M.; Levantino, M.; Schotte, F.; Anfinrud, P. A.; Ewald, F.; Choi, J.; Cupane, A.; Wulff, M.; Ihee, H. *Nat. Methods* **2008**, *5*, 881.
(12) Cho, H. S.; Dashdorj, N.; Schotte, F.; Graber, T.; Henning, R.; Anfinrud, P. *Proc. Natl. Acad. Sci. U.S.A.* **2010**, *107*, 7281.
(13) Kern, J.; Alonso-Mori, R.; Hellmich, J.; Tran, R.; Hattne, J.; Laksmono, H.; Glöckner, C.; Echols, N.; Sierra, R. G.; Sellberg, J.; Lassalle-Kaiser, B.; Gildea, R. J.; Glatzel, P.; Grosse-Kunstleve, R. W.; Latimer, M. J.; McQueen, T. A.; DiFiore, D. R.; Fry, A. R.; Messerschmidt, M.; Miahnahri, A.; Schafer, D. W.; Seibert, M. M.; Sokaras, D.; Weng, T.-C.; Zwart, P. H.; White, W. E.; Adams, P. D.; Bogan, M. J.; Boutet, S. B.; Williams, G. J.; Messinger, J.; Sauter, N. K.; Zouni, A.; Bergmann, U.; Yano, J.; Yachandra, V. K. *Proc. Natl. Acad. Sci. U.S.A.* **2012**, *109*, 9721.
(14) Jung, Y. O.; Lee, J. H.; Kim, J.; Schmidt, M.; Moffat, K.; Šrajer, V.; Ihee, H. *Nat. Chem.* **2013**, *5*, 212.
(15) Hamm, P.; Lim, M. H.; Hochstrasser, R. M. *J. Phys. Chem. B* **1998**, *102*, 6123.
(16) Hamm, P.; Lim, M.; DeGrado, W. F.; Hochstrasser, R. M. *Proc. Natl. Acad. Sci. U.S.A.* **1999**, *96*, 2036.
(17) Asplund, M. C.; Zanni, M. T.; Hochstrasser, R. M. *Proc. Natl. Acad. Sci. U.S.A.* **2000**, *97*, 8219.
(18) Volk, M. *Eur. J. Org. Chem.* **2001**, 2605.
(19) Kolano, C.; Helbing, J.; Kozinski, M.; Sander, W.; Hamm, P. *Nature* **2006**, *444*, 469.
(20) Lu, H. S. M.; Volk, M.; Kholodenko, Y.; Gooding, E.; Hochstrasser, R. M.; DeGrado, W. F. *J. Am. Chem. Soc.* **1997**, *119*, 7173.
(21) Volk, M.; Kholodenko, Y.; Lu, H. S. M.; Gooding, E. A.; DeGrado, W. F.; Hochstrasser, R. M. *J. Phys. Chem. B* **1997**, *101*, 8607.
(22) Rock, R. S.; Chan, S. I. *J. Org. Chem.* **1996**, *61*, 1526.
(23) Rock, R. S.; Chan, S. I. *J. Am. Chem. Soc.* **1998**, *120*, 10766.
(24) Hansen, K. C.; Rock, R. S.; Larsen, R. W.; Chan, S. I. *J. Am. Chem. Soc.* **2000**, *122*, 11567.
(25) Chen, R. P. Y.; Huang, J. J. T.; Chen, H. L.; Jan, H.; Velusamy, M.; Lee, C. T.; Fann, W. S.; Larsen, R. W.; Chan, S. I. *Proc. Natl. Acad. Sci. U.S.A.* **2004**, *101*, 7305.
(26) Milanesi, L.; Waltho, J. P.; Hunter, C. A.; Shaw, D. J.; Beddard, G. S.; Reid, G. D.; Dev, S.; Volk, M. *Proc. Natl. Acad. Sci. U.S.A.* **2012**, *109*, 19563.
(27) Tucker, M. J.; Courter, J. R.; Chen, J.; Atasoylu, O.; Smith, A. B., III; Hochstrasser, R. M. *Angew. Chem., Int. Ed.* **2010**, *49*, 3612.
(28) Tucker, M. J.; Abdo, M.; Courter, J. R.; Chen, J.; Smith, A. B., III; Hochstrasser, R. M. *J. Photochem. Photobiol., A* **2012**, *234*, 156.
(29) Abdo, M.; Brown, S. P.; Courter, J. R.; Tucker, M. J.; Hochstrasser, R. M.; Smith, A. B., III. *Org. Lett.* **2012**, *14*, 3518.
(30) Tucker, M. J.; Abdo, M.; Courter, J. R.; Chen, J.; Brown, S. P.; Smith, A. B., III; Hochstrasser, R. M. *Proc. Natl. Acad. Sci. U.S.A.* **2013**, *110*, 17314.
(31) Marqusee, S.; Robbins, V. H.; Baldwin, R. L. *Proc. Natl. Acad. Sci. U.S.A.* **1989**, *86*, 5286.
(32) Verdine, G. L.; Hilinski, G. J. *Methods Enzymol.* **2012**, *503*, 3.
(33) Chakrabartty, A.; Kortemme, T.; Baldwin, R. L. *Protein Sci.* **1994**, *3*, 843.
(34) Luo, P. Z.; Baldwin, R. L. *Biochemistry* **1997**, *36*, 8413.
(35) Barlos, K.; Gatos, D.; Koutsogianni, S. *J. Pept. Res.* **1998**, *51*, 194.
(36) Subiros-Funosas, R.; Prohens, R.; Barbas, R.; El-Faham, A.; Albericio, F. *Chem.—Eur. J.* **2009**, *15*, 9394.
(37) Frisch, M. J.; Trucks, G. W.; Schlegel, H. B.; Scuseria, G. E.; Robb, M. A.; Cheeseman, J. R.; Scalmani, G.; Barone, V.; Mennucci, B.; Petersson, G. A.; Nakatsuji, H.; Caricato, M.; Li, X.; Hratchian, H. P.; Izmaylov, A. F.; Bloino, J.; Zheng, G.; Sonnenberg, J. L.; Hada, M.; Ehara, M.; Toyota, K.; Fukuda, R.; Hasegawa, J.; Ishida, M.; Nakajima, T.; Honda, Y.; Kitao, O.; Nakai, H.; Vreven, T.; Montgomery, J. A., Jr.; Peralta, J. E.; Ogliaro, F.; Bearpark, M.; Heyd, J. J.; Brothers, E.; Kudin, K. N.; Staroverov, V. N.; Kobayashi, R.; Normand, J.; Raghavachari, K.; Rendell, A.; Burant, J. C.; Iyengar, S. S.; Tomasi, J.; Cossi, M.; Rega, N.; Millam, N. J.; Klene, M.; Knox, J. E.; Cross, J. B.; Bakken, V.; Adamo, C.; Jaramillo, J.; Gomperts, R.; Stratmann, R. E.; Yazyev, O.; Austin, A. J.; Cammi, R.; Pomelli, C.; Ochterski, J. W.; Martin, R. L.; Morokuma, K.; Zakrzewski, V. G.; Voth, G. A.; Salvador, P.; Dannenberg, J. J.; Dapprich, S.; Daniels, A. D.; Farkas, Ö.; Foresman, J. B.; Ortiz, J. V.; Cioslowski, J.; Fox, D. J. *Gaussian 09*, revision D.01; Gaussian, Inc.: Wallingford, CT, 2009.
(38) Torres, J.; Adams, P. D.; Arkin, I. T. *J. Mol. Biol.* **2000**, *300*, 677.
(39) Torres, J.; Kukol, A.; Goodman, J. M.; Arkin, I. T. *Biopolymers* **2001**, *59*, 396.
(40) Fang, C.; Wang, J.; Charnley, A. K.; Barber-Armstrong, W.; Smith, A. B., III; Decatur, S. M.; Hochstrasser, R. M. *Chem. Phys. Lett.* **2003**, *382*, 586.
(41) Fang, C.; Wang, J.; Kim, Y. S.; Charnley, A. K.; Barber-Armstrong, W.; Smith, A. B., III; Decatur, S. M.; Hochstrasser, R. M. *J. Phys. Chem. B* **2004**, *108*, 10415.
(42) Fang, C.; Hochstrasser, R. M. *J. Phys. Chem. B* **2005**, *109*, 18652.
(43) Marecek, J.; Song, B.; Brewer, S.; Belyea, J.; Dyer, R. B.; Raleigh, D. P. *Org. Lett.* **2007**, *9*, 4935.
(44) Remorino, A.; Korendovych, I. V.; Wu, Y.; DeGrado, W. F.; Hochstrasser, R. M. *Science* **2011**, *332*, 1206.
(45) Remorino, A.; Hochstrasser, R. M. *Acc. Chem. Res.* **2012**, *45*, 1896.